SPEEDAM 2004 June 16th – 18th, CAPRI (Italy)

AXIAL FLUX, FIELD REGULATED PM SYNCHRONOUS GENERATORS WITH CONCENTRATED ARMATURE WINDINGS

Antonino Di Gerlando, Roberto Perini, Mario Ubaldini

Dipartimento di Elettrotecnica, Politecnico di Milano, Piazza L. da Vinci, 32 – 20133 Milano, Italy
antonino.digerlando@polimi.it; roberto.perini@polimi.it; mario.ubaldini@polimi.it

Abstract

Some novel design structures of PM, axial flux, synchronous generators are presented, employing armature windings consisting of concentrated coils wounded around the stator teeth; the voltage control is based on the variation of the windings flux linkage, obtained by modifying the stator (or rotor) double sided configuration. Thanks to the high number of poles and the excellent waveform quality, this kind of machine is well suited for hydro or wind generators. In the paper, the main constructive machine features are discussed, together with some design and FEM results.

1.- INTRODUCTION

Recently, a great interest has grown towards PM electrical machines equipped with concentrated coils, thanks to their conspicuous constructional and functional advantages (mainly an easier machine manufacture and the development of high torques and e.m.f.s at low speed).
Several types have been developed: cylindrical air-gap configurations, with modular E-shaped cores [1, 2, 3], or machines with uniformly toothed stator structure [4, 10, 11, 12]; flat air-gap machines [5] and structures using Soft Magnetic Composites [6]; solutions with non-uniform slotting dispositions [7, 8, 9].
The usual limits of these solutions concern e.m.f. waveform quality and regulation and torque ripple: in order to face these problems, some field regulated, PM machines have been already considered [13], employing auxiliary d.c. coils; besides, the variation of teeth and poles heads extension has been proposed, or the use of unequal pole pitches, while a general approach to the concentrated winding theory seems not completely developed yet.
In the paper, some PM, axial flux machines are considered, whose armature windings are equipped with two-layer concentrated coils, in the following also called "tooth coils" [14, 15]. Moreover, some dispositions are analysed, allowing the field variation: in fact, here the regulation is obtained without auxiliary field currents, but just by applying suited small rotational displacements among machine portions.

2.- GENERAL FEATURES OF CONCENTRATED WINDING PM SYNCHRONOUS MACHINES

Common characteristics of the tooth-coil machines considered in this paper are (see figures 1 and 2):
– uniformly distributed magnetic structures of stator armature and rotor inductor (each structure has equally shaped saliencies - teeth and PMs -);
– tooth pitch τ_t and PM pitch τ_m almost equal (it can be $\tau_m<\tau_t$ or $\tau_m>\tau_t$, but $\tau_m \neq \tau_t$);
– series inverted connection of coils belonging to adjacent teeth of the same phase (controverse coils).

By adopting the representation of fig.1-right to specify the winding sense of each coil, a typical three-phase, two-layer winding appears as in fig.2 (no hypotheses are assumed for now about the armature yoke disposition).
Referring to fig.2, the following quantities and properties can be considered:

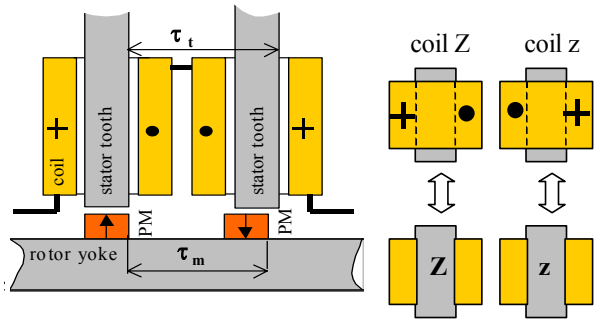

Fig.1 - Left: basic structure of a PM synchronous machine, equipped with tooth coil armature winding.
Right: coil winding senses around teeth.

– cycle: space period, i.e. periphery portion at which bounds the faced structures repeat the same reciprocal disposition among PMs and teeth;
– cycle-phase: referring to a layer, portion of one cycle including adjacent coils belonging to the same phase;
– parent coil: for each layer, the first coil of every cycle-phase, whose full succession describes the winding;
– the N° of teeth/cycle N_{tc} and the N° of armature coils/cycle N_{cc} are multiple of the N° of phases N_{ph};
– links among teeth N°/cycle-phase N_{tcph} and coils N° /cycle-phase N_{ccph}: $N_{tc}= N_{ph}\cdot N_{tcph}$; $N_{cc}= N_{ph}\cdot N_{ccph}$;
– in case of controverse coils, the N° of coils /cycle-phase N_{ccph} equals the N° of teeth /cycle-phase N_{tcph};
– the N° of coils /cycle-phase N_{ccph} can be any integer;
– the optimal N° of PMs/cycle N_{mc} differs by one with respect to N_{tc}: $N_{mc} = N_{tc} \pm 1$ (this choice gives highest winding factor and lowest harmonic distortion);
– the optimal displacement among layers equals a N° of teeth N_{ts} as near as possible $N_{ccph}/2$;
– all cycles are identical: thus, the N° of cycles N_c equals the max N° of parallel paths of every phase;
– the total N° of PMs $N_m = N_{mc}\cdot N_c$ of a rotating machine must be even; thus, if N_{mc} is even, N_c can be any integer; if N_{mc} is odd, N_c must be even;
– it can be shown that the winding factor k_w of a three-phase tooth-coil machine with fixed configuration (having double-layer windings, N_{ccph} coils/(cycle-phase)), N_{tcph} teeth/(cycle-phase) and layer displacement of N_{ts} teeth, see fig.2) equals the product of a distribution factor k_d times a layer displacement factor k_s; for the k^{th} harmonic e.m.f. (k = 1, 3, 5,…) it is:

$$k_{w_k} = k_{d_k} \cdot k_{s_k} \,, \qquad (1)$$

$$\text{with} \quad k_{d_k} = \frac{\sin\left(k\cdot\pi/6\right)}{N_{ccph}\cdot\sin\left[\left(k/N_{ccph}\right)\cdot\pi/6\right]} \,, \qquad (2)$$

$$k_{s_k} = \cos\left(k\cdot\left(N_{ts}/N_{tcph}\right)\cdot\pi/6\right) \,; \qquad (3)$$

as known, a traditional machine, with two layers, distributed windings, q slots/(pole-phase) and coil pitch shortening of c_a slots, exhibits a winding factor f_a equal to the product of a distribution factor f_d times a pitch factor f_p, with expressions exactly corresponding to the previous ones, provided that we associate N_{ccph} with q, and N_{ts} with c_a: the difference is that, with a traditional machine, a good e.m.f. waveform quality and a low cogging and torque ripple can be obtained by adopting at least $q \approx 5$, while a tooth coil machine exhibits similar performance quality with $q \approx 0.33$;
– the orders "k_{th}" of e.m.f. tooth harmonics (with the same winding factor of the principal e.m.f.) equal:

$$k_{th} = \nu\cdot 6\cdot N_{ccph} \mp 1 \,, \quad \nu = 1,2,3,... \qquad (4)$$

The main advantages in using these machines in the wind or hydro power generation sectors are:
– the magnetic and winding arrangements allow to obtain high N° of poles, thanks to the very low q values;
– the stator manufacture is simplified: no skewing is required; only concentrated coils are used; moreover, in case of absence of teeth head shoes, the coils can be prepared separately; the endwindings overlapping is avoided, with reduced copper mass and stator losses;
– even at low rotational speed, the frequency is adequate, allowing the turbine - generator direct coupling.

3.- STRUCTURE AND FIELD REGULATION OF AXIAL FLUX PM GENERATORS

Fig. 3 shows the basic structure of two kinds of axial flux, field regulated PM generators: just two coils are represented. In both structures, the armature winding is based on a "two layers" principle and it is assumed with controverse coils ($N_{ccph} = N_{tcph}$): each tooth has one coil/tooth in case of a double stator machine, two coils/tooth in case of a double rotor machine.
As depicted in fig.3 (see empty arrows), the field control (thus, the voltage regulation) is obtained by applying a

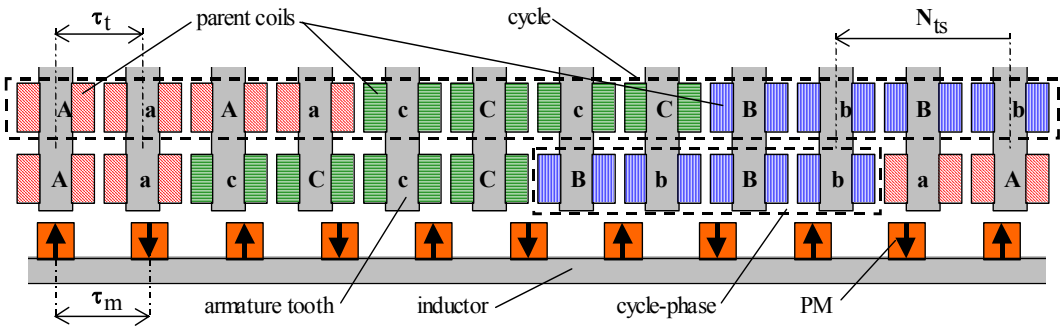

Fig.2 - Double layer winding (2 coils/tooth), with controverse tooth coils: $N_{tc} = 12$; $N_{cc} = 12$; $N_{ph} = 3$; $N_{tcph} = N_{ccph} = 4$; $N_{ts} = 2$.

small rotational displacement among the external, twin structures. In spite of the configuration similarities, significant differences exist between the two structures:

– in the double stator structure, the rotational displacement must be applied among stationary structures; moreover, the single tooth-coil flux waveform is not affected by the displacement, whilst the corresponding electrical displacement angle between stators implies a variable phasor resultant of the tooth coil e.m.f.s;
– in the double rotor structure, the displacement must be applied among rotating elements, thus requiring a differential device similar to those used in the cars; besides, the winding e.m.f. varies because each tooth flux waveform is modified by the displacement itself.

The double stator structure is more widely known, even if frequently used with distributed winding machines; on the contrary, the double rotor one is more unusual, especially for the absence of the armature core yoke.

Fig.4 shows the constructed stator of a double rotor machine, whose teeth are fixed on a supporting frame.

Just as a first indication of regulation possibilities and waveform quality, fig.5 shows the FEM simulated [16] no-load line-to-line e.m.f. waveform $e_{o\ell}(t)$ of a double stator machine, with the regulation ratio ρ_τ as parameter:

$$\rho_\tau = \Delta x / \tau_a \ , \qquad (5)$$

where Δx is the reciprocal peripheral displacement among the stators and τ_a the armature tooth pitch.

Referring to the sizes of fig.3-left, the main data of the analysed machine are summarised in Table I.

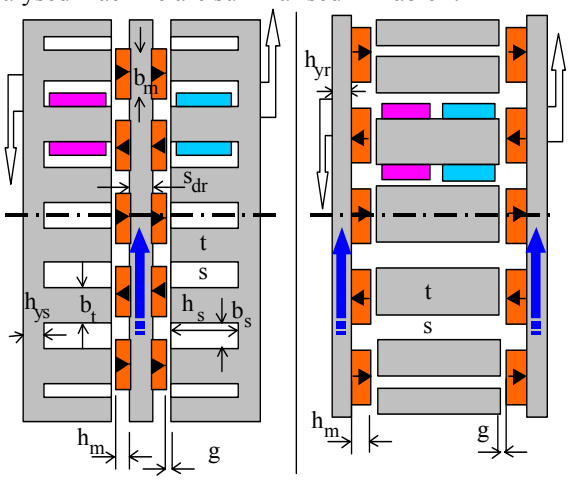

Fig.3 – Magnetic structures of double sided, axial flux, tooth-coil, PM machines (shaft not shown; only two coils depicted); left: double stator machine; right: double rotor machine. Solid arrows = sense of the rotor movement; empty arrows = reciprocal rotation among the external twin structures, in order to obtain the field regulation (the figure layout shows the aligned disposition of the twin external structures).

Fig.4 – Wounded stator magnetic structure of a double rotor, axial flux, flat air-gap, PM machine, equipped with concentrated coils (N_c= 2; N_{ph}= 3; N_{tcph}= 6; N_{ts}= 3; D_{int}= 500 mm).

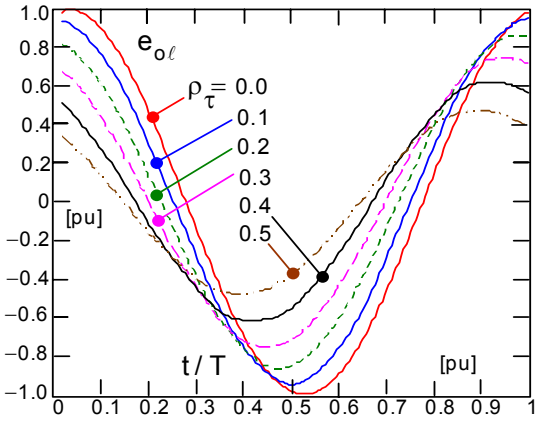

Fig.5 – FEM calculated no-load line-to-line e.m.f. waveforms of a PM generator (data of Table I; p.u. values, referred to the peak value of the max. e.m.f.); $\rho_\tau = \Delta x / \tau_a$ = regulation ratio (p.u. rotational displacement among stators).

Table I – Main data of the double stator PM generator considered in the simulations (see size symbols in fig.3, left)

PM material: NdFeB: B_r [T]; H_{cB} [kA/m]	1.23; 890
PM sizes: b_m; h_m; radial size d_m [mm]	20; 10; 70
Number of PM N_m and teeth N_t (per side)	38; 36
Cycles N_c; layer displacement N_{ts}; N_{ph}	2; 3; 3
Core internal diameter D_i; air-gap g [mm]	500; 1.5
Core sizes: b_s, h_s; b_{tav}; h_{ys}; s_{dr} [mm]	33; 60; 17; 10; 8

The following remarks are valid:

– a small displacement is sufficient in order to obtain an important voltage regulation (in the example of fig.5 ρ_τ = 0.5 corresponds to 5° mechanical degrees);
– for any value of the displacement ratio ρ_τ, the waveform remains substantially sinusoidal.

4.- NO-LOAD VOLTAGE ANALYSIS

In the following, a quantitative analysis will be performed, concerning field regulation and variation of the no-load voltage amplitude and harmonic content, based on a phasor approach and on FEM simulations.

At first, the double stator machine will be considered. For this machine, the basic no-load quantity is the tooth flux time waveform $\varphi_t(t)$: in fact, assuming negligible saturation, $\varphi_t(t)$ depends only on the machine structure and it is the same for all teeth, regardless the reciprocal displacement among the stators.

The tooth flux waveform follows from magneto-static FEM simulations; in fact, observing that, at constant angular frequency ω, $\theta = \omega \cdot t$ occurs, $\varphi_t(\theta)$ can be evaluated instead of $\varphi_t(t)$, by numerically sampling a sufficiently high N° of electrical rotor angles θ within a double PM pitch rotation. By performing a Fourier series analysis of $\varphi_t(\theta)$, the peak tooth flux harmonic components Φ_{t_k} can be obtained, thus allowing the evaluation of the RMS values of the tooth e.m.f. (E_{t_k}) and of the resultant phase e.m.f. of each of the two stators (E_{s_k}):

$$E_{t_k} = \omega \cdot \Phi_{t_k} / \sqrt{2} \qquad (6)$$

$$E_{s_k} = E_{t_k} \cdot N_{tu.co} \cdot N_{ccph} \cdot (N_c/a) \cdot k_{d_k} \quad , \qquad (7)$$

with $N_{tu.co}$ N° of turns/coil and "a" N° of parallel paths (sub-multiple of -or equal to- N_c). In order to obtain the expression of the line-to-neutral harmonic e.m.f. E_k at the machine terminals, the phasor diagram of fig.6 should be considered, in which ϑ_{s_k} is the resultant electrical angle among the two winding axes of the same phase, belonging to the twin stators.

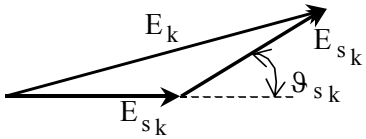

Fig.6 – Phasor diagram of the phase harmonic e.m.f. of each stator winding (E_{s_k}) and of the machine line-to-neutral e.m.f. (E_k), as a function of the electrical angle (ϑ_{s_k}) among the two winding axes of the same phase, belonging to the twin stators.

The angle ϑ_{s_k} includes the layer displacement angle $\vartheta_{s\ell_k}$ and the field regulation angle ϑ_{sr_k}:

$$\vartheta_{s_k} = \vartheta_{s\ell_k} + \vartheta_{sr_k} , \qquad (8)$$

while the line-to-neutral e.m.f. E_k equals:

$$E_k = 2 \cdot E_{s_k} \cdot \cos(\vartheta_{s_k}/2) . \qquad (9)$$

The layer displacement angle $\vartheta_{s\ell_k}$ is:

$$\vartheta_{s\ell_k} = k \cdot N_{ts} \cdot \frac{\pi \cdot N_{mc}}{N_{tc}} \quad ; \qquad (10)$$

considering that $N_{mc} = N_{tc} \pm 1$, $N_{ph} = 3$, (10) becomes:

$$\vartheta_{s\ell_k} = k \cdot N_{ts} \cdot \pi \cdot \left(1 \pm 1/(3 \cdot N_{tcph})\right) . \qquad (11)$$

The field regulation angle ϑ_{sr_k} is:

$$\vartheta_{sr_k} = k \cdot \rho_\tau \cdot \frac{\pi \cdot N_{mc}}{N_{tc}} \quad ; \qquad (12)$$

in the same hypotheses used for (10), (12) becomes:

$$\vartheta_{sr_k} = k \cdot \rho_\tau \cdot \pi \cdot \left(1 \pm 1/(3 \cdot N_{tcph})\right) . \qquad (13)$$

Finally, choosing $N_{mc} = N_{tc} + 1$, and considering that any multiple of π does not affect the amplitude of the result, from (9) we obtain:

$$E_k = 2 \cdot E_{s_k} \cdot k_{r_k}(\rho_\tau) , \quad \text{where} \qquad (14)$$

$$k_{r_k}(\rho_\tau) = \left| \cos\left(k \cdot \frac{\pi}{2} \cdot \left(\frac{N_{ts}/3}{N_{tcph}} + \rho_\tau \cdot \left(1 + \frac{1/3}{N_{tcph}} \right) \right) \right) \right| \qquad (15)$$

is the regulation factor; $k_{r_k}(\rho_\tau)$ becomes the displacement factor k_s of (3) for $\rho_\tau = 0$.

For k = 1, from (15) the value $\rho_{\tau o}$ of the regulation ratio, that makes zero the fundamental e.m.f., follows:

$$\rho_{\tau o} = 1 - \frac{N_{ts} + 1}{3 \cdot N_{tcph} + 1} \quad . \qquad (16)$$

Eq. (16) confirms the limited displacement rotation between stators required to regulate the voltage ($\rho_{\tau o} < 1$).

In order to estimate the effects of the field regulation on the fundamental and on the higher order harmonic e.m.f.s, it is worth to analyze the behaviour of the regulation winding factor, $k_{wr_k}(\rho_\tau)$:

$$k_{wr_k}(\rho_\tau) = k_{d_k} \cdot k_{r_k}(\rho_\tau) . \qquad (17)$$

The following remarks can be made (see fig.7):

- the fundamental winding factor varies, according to a regular and almost linear law, with the ρ_τ variation;
- of course, the following occurs: $k_{wr_k}(\rho_\tau = 0) = k_{w_k}$;
- the 3rd and 9th harmonic winding factors are significant, but they affect just the phase-to-neutral e.m.f., whilst the usual adopted output is the line-to-line one;
- the higher harmonic winding factors remain always limited; in any case, their actual effect depends also on the corresponding harmonic tooth flux amplitudes.

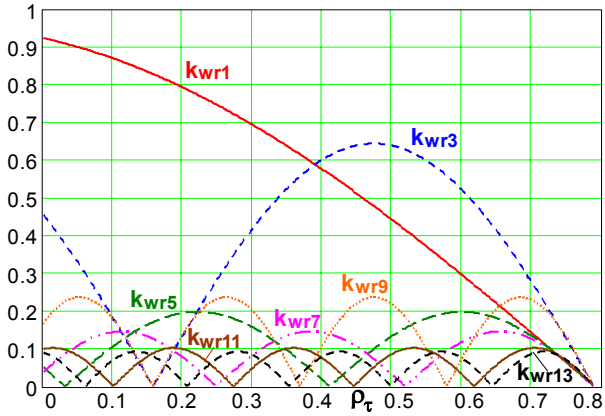

Fig.7 – Regulation winding factor (see (17)), showing the modulation of fundamental and harmonic winding factors as a function of the regulation ratio ρ_τ (same data of fig.5).

Figures 8, 9 show the calculated amplitude of the fundamental and higher harmonic phase-to-neutral no-load e.m.f.s of the machine of Table I, as a function of $\rho\tau$: all the curves are expressed in p.u., referred to the fundamental harmonic rms value $E1_M$, occurring for $\rho\tau = 0$.
The curves represent the values obtained by (6) and (7) (with Φt_k calculated by FEM), while the points are directly evaluated by FEM as winding flux linkage.

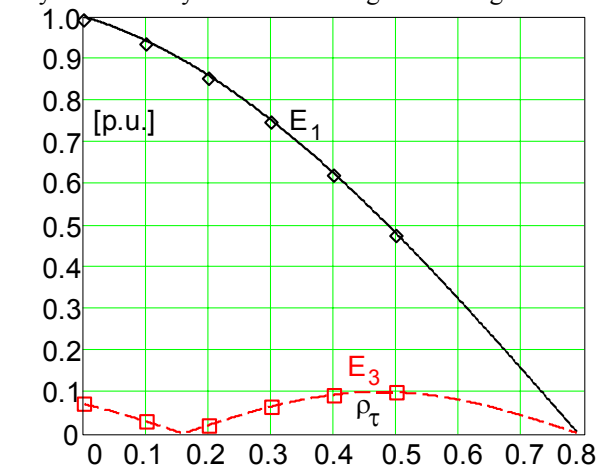

Fig.8 – p.u. fundamental and 3rd harmonic phase-to-neutral no-load e.m.f. of the machine of Table I, as a function of $\rho\tau$: all the curves are expressed in p.u., referred to the fundamental harmonic rms value $E1_M$, occurring for $\rho\tau = 0$.
Curves= values obtained by (6) and (7) (with Φt_k calculated by FEM); points= calculated by FEM as winding flux linkage.

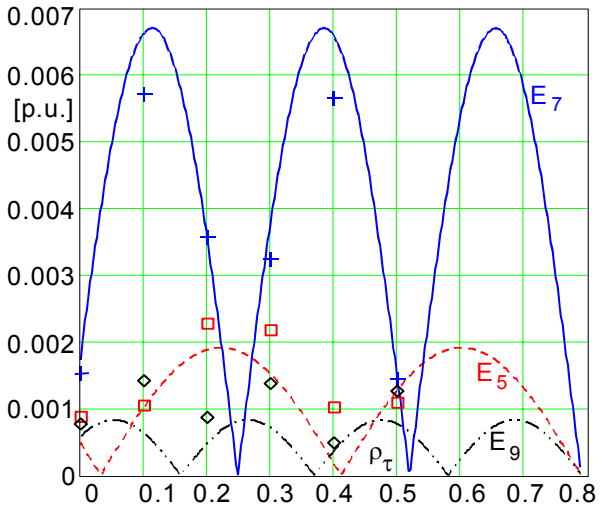

Fig.9 – 5th, 7th and 9th harmonic phase-to-neutral no-load e.m.f. of the machine of Table I: same conditions of fig.8.

The following remarks are valid:

– the excellent congruence concerning the fundamental and the 3rd harmonic validates (6) and (7);
– the 3rd harmonic reaches significant values, but it does not affect the line-to-line e.m.f.; as known, the same occurs for all the harmonics multiple of the 3rd one;
– the higher discrepancies of fig.9 are due to the very small e.m.f. values, that imply significant numerical errors in the FEM evaluated winding flux linkage.

A global index of the waveform distortion level is the Total Harmonic Distortion; fig.10 shows the $THD_{E\ell}$ of the line-to-line e.m.f., evaluated as follows:

$$THD_{E_\ell} = \sqrt{\sum_k E_k^2(\rho_\tau)} \Big/ E_1(\rho_\tau), \quad k = 5,7,11,\ldots 39. \quad (18)$$

The distortion remains of the order of 1% all along the interval $0 \le \rho\tau \le 0.5$, that is the most relevant range for the regulation; on the other hand, for higher $\rho\tau$ values the THD p.u. value increases, but E_1 tends to zero.

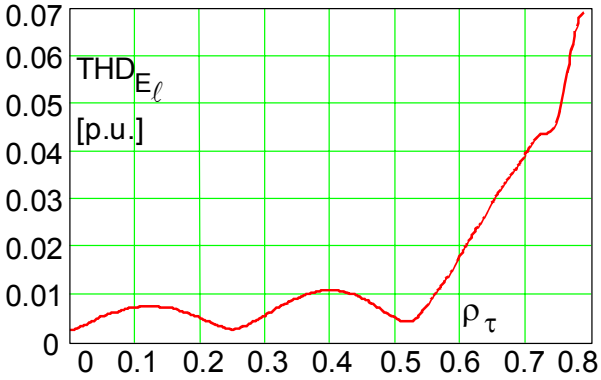

Fig.10 – Total harmonic distortion of the line-to-line no-load e.m.f. of the machine of Table I, as a function of $\rho\tau$: $THD_{E\ell}(\rho\tau)$ is referred to the actual $E_1(\rho\tau)$ value.

Evaluations similar to the previous ones have been performed also for the double rotor PM generator (fig.3, right): with the same sizes of Table I, the obtained results are analogous to those of fig.s from 5 to 10.
Just to show the behaviour due to the different variation of the tooth flux waveform as a function of $\rho\tau$, fig.11 shows the fundamental no-load e.m.f.s for the double stator (E_{ds1}) and double rotor (E_{dr1}) generators.

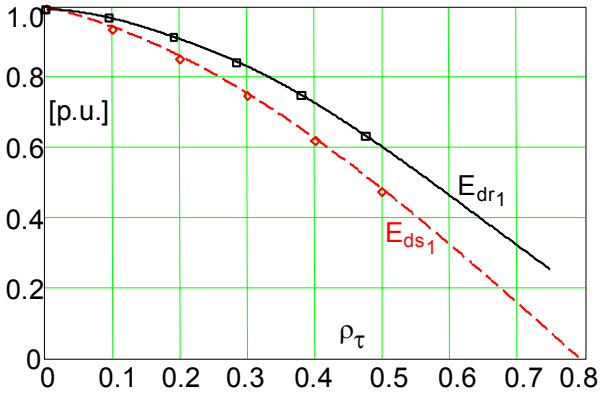

Fig.11 – Fundamental no-load e.m.f.s for the double stator (E_{ds1}) and double rotor (E_{dr1}) generators: curves= values obtained by (6) and (7) (with Φt_k by FEM); points= evaluated by FEM as winding flux linkage.

As before, the curves are based on (6) and (7) (with Φ_{tk} by FEM), while the points are evaluated by FEM as winding flux linkage: the double rotor machine presents a weaker dependence on the regulation ratio, compared with the double stator generator.

5.- STEADY-STATE LOADED OPERATION

As known, the V(I) characteristics of a PM generator is influenced by the equivalent series impedance, including phase resistance R and synchronous reactance X.
Disregarding the winding resistance (inherently constant and weakly contributing to the impedance), the question to answer is the level of anisotropy of the machine and the dependence of the reactance on the regulation ratio $\rho\tau$. Several FEM simulations have been performed to evaluate X on both the machine structures of fig.3, always according to the following criteria:

- PMs transformed in passive components (unvaried reversible permeability: $\mu_r \approx 1.1$; zero remanence);
- phases winding supplied by d.c. currents with zero sum ($I_A = I$; $I_B = I_C = -0.5 \cdot I$), thus obtaining a reaction m.m.f. aligned along the phase A axis;
- FEM calculation of machine magnetic energy, both in "d" and "q" alignment positions.

All the analyses have shown a very weak level of anisotropy (differences of few percent among X_d and X_q) and null dependence of the reactance on $\rho\tau$.
Thus, for design and operation purposes, the model of the described field regulated PM generators should be considered as follows: the machine is isotropic, with constant synchronous reactance; the rated no-load voltage should be chosen around the $\rho\tau \approx 0.5$ condition, in such a way to maintain the terminal voltage constant at loaded operation, by using a sufficient regulation range of $\rho\tau$, in order to compensate the armature reaction.

6.- CONCLUSION

Some novel configurations of PM axial flux synchronous generators have been presented, capable of field regulation without auxiliary excitation windings.
Some original double-layer winding configurations have been presented and analyzed, together with the dependence of the no-load e.m.f. waveform quality and of the reactance on the field regulation, consisting in a small rotational displacement among the external, twin structures of the machine.
The encouraging simulation results stimulate further research activities, both from the theoretical and from the experimental point of view.

REFERENCES

[1] Spooner, E.; Williamson, A. C.: *Direct coupled, PM generators for wind turbine applications*, IEE Proc. El. Power Appl., V.143, N.1, Jan. 96, pp.1-8.

[2] Spooner, E.; Williamson, A. C.; Catto, G.: *Modular design of PM generators for wind turbines*, ibidem, V.143, N.5, Sept. 96, pp.388-395.

[3] Spooner, E.; Williamson, A. C.: British Patent Application 2278738, "Modular Electromagnetic Machine".

[4] Lampola, P.: *Electromagnetic Design of an Unconventional Directly Driven PM Wind Generator*, Proc.ICEM'98, Istanbul, pp.1705-1710.

[5] Lukaniszyn, M.; Jagiela, M.; Wrobel, R.: *Influence of Magnetic Circuit Modifications on the Torque of a Disc Motor with Co-axial Flux in the Stator*, Proc. ICEM '02, Brugge, Belgium, paper N° 069.

[6] Muetze, A.; Jack, A.; Mecrow, B.: *Alternate Designs of Low Cost Brushless DC Motors using Soft Magnetic Composites*, ibid., paper N° 237.

[7] Koch, Th.; Binder, A.: *PM Machines with Fractional Slot Winding for Electric Traction*, ibidem, paper N° 369.

[8] Tounsi, S.; Gillon, F.; Brisset, S.; Brochet, P.; Neji, R.: *Design of an axial flux brushless DC motor for electric vehicle*, ibidem, paper N° 581.

[9] Canders, W.; Laube, F.; Mosebach, H.: *PM Excited Polyphase Synchronous Machines with Single-Phase Segments. Featuring Simple Tooth Coils*, ib., paper N° 610.

[10] Magnussen, F.; Sadurangani, C.: *Winding Factors and Joule Losses of PM Machines with Concentrated Windings*, IEEE-IEMDC '03 Conf. Proc., Madison, Wisconsin, USA, 1-4 June 2003, pp.333-339.

[11] Bianchi, N.; Bolognani, S.; Luise, F.: *Analysis and Design of a Brushless Motor for High Speed Operation*, ibidem, pp.44-51.

[12] Bianchi, N.; Bolognani, S.; Frare, P.: *Design Criteria of High η SPM Synchronous Motors*, ibid., pp.1042-1048.

[13] Tapia, J. A.; Aydin, M.; Huang, S.; Lipo, T. A.: *Sizing Equation Analysis for Field Controlled PM Machines: A Unified Approach*, ibidem, pp.1111-1116.

[14] Di Gerlando, A.; Ubaldini, M.: Italian Patent Application MI2002A 001186, "Synchronous Electrical Machine with Concentrated Coils", May 31st, 2002; International PCT Patent pending.

[15] Di Gerlando, A.; Perini, R.; Ubaldini, M.: *Permanent Magnet Linear Actuators with Concentrated Coils*, 4th Intern. Symp. on Linear Drives for Industry Appl., LDIA 2003, Birmingham, UK, 8-10 Sept. 2003, pp.371-374.

[16] Maxwell 2D and 3D FEM codes, v.10, Ansoft Corporation, Pittsburgh, PA, USA, Nov. 2003.